ARTICLE

Modification of Reflectron Time-of-Flight Mass Spectrometer for Photodissociation of Mass-Selected Cluster Ions†

Yu-chao Zhao, Zeng-guang Zhang, Jin-yun Yuan, Hong-guang Xu, Wei-jun Zheng*

Beijing National Laboratory for Molecular Science, State Key Laboratory of Molecular Reaction Dynamics, Institute of Chemistry, Chinese Academy of sciences, Beijing 100190, China

(Dated: Received on October 31, 2009; Accepted on November 13, 2009)

We introduce a modification of reflectron time-of-flight mass spectrometer for laser photodissociation of mass-selected ions. In our apparatus, the ions of interests were selected by a mass gate near the first space focus point and decelerated right after the mass gate, were then crossed by a laser beam for dissociation. The daughter ions and surviving parent ions were re-accelerated and analyzed by the reflectron time-of-flight mass spectrometer. Compared to the designs reported by other research groups, our selection-deceleration-dissociation-reacceleration approach has better daughter-parent-ions-separation, easier laser timing, and better overlapping between the ion beam and laser beam. We also conducted detailed calculations on the parent ion and daughter ion flight times, and provided a simplified formula for the calibration of daughter ion mass.

Key words: Reflectron time-of-flight mass spectrometer, Photodissociation, Mass-selection, Cluster

I. INTRODUCTION

Reflectron time-of-flight mass spectrometer has much better mass-resolution than linear time-of-flight mass spectrometer [1]. Therefore, the technique of reflectron time-of-flight mass spectrometer has been used extensively in chemical physics experiments, such as multiphoton ionization [2−6], photodesorption [7], and photodissociation experiments [8−17]. This technique is especially useful to photodissociation experiments of cluster ions. It has been used to study the photodissociation dynamics of atomic cluster ions [18] and to investigate IR photodissociation spectra of cluster ions formed by metal and small molecules such as CO, O, benzene, H_2O, N_2, CO_2, etc. [19−25]. It has also been utilized to explore the ultrafast dissociation dynamics of neutral species through electron photodetachment from precursor anions [26].

We notice that many research groups conducted photodissociation experiments by crossing the laser beam with the ion beam at the turning point of their reflectron time-of-flight mass spectrometer [27−30]. There are several disadvantages with this type of setup. First, the flight distance of the daughter ions is very short in this type of setup. Thus, the mass resolution of daughter ions is relatively poor although the parent ion mass resolution is splendid. The daughter ions and parent ions cannot be separated very well. Second, the ions packs spread quite broadly at the turning point while the laser beams are usually small with diameter smaller than 1 cm. Therefore, this method cannot grant good overlap between the ion pack and laser beam. Third, the best location for mass selection is at the first space focus point of the apparatus which is far away from the turning point. That makes it difficult to determine the photodissociation laser time based on the mass gate time. In the setups reported by Bouyer *et al.* [18] and Lineberger group [26], the laser beams crossed the ion beams near the mass gate without deceleration and reacceleration processes. Therefore, the daughter ion kinetic energy is relatively lower than the parent ion kinetic energy. That could not grant good separation between the daughter ions and parent ions.

In this paper, we introduce a new approach to avoid the above disadvantages. We name it selection-deceleration-dissociation-reacceleration method. With this method, the mass-selection and photodissociation regions are all near the first space focus point. This arrangement is not only convenient for determining the fire time of the photodissociation laser, but also helpful to reduce the background noise. In addition, we decelerate the parent ions before dissociation and reacceleration both parent ions and daughter ions after dissociation. That can improve the mass separation of the daughter ions and parent ions.

†Part of the special issue for "the Chinese Chemical Society's 11th National Chemical Dynamics Symposium".

*Author to whom correspondence should be addressed. E-mail: zhengwj@iccas.ac.cn

II. OVERVIEW OF THE EXPERIMENTAL SETUP

Our experimental setup is modified from an old machine which has been reported previously [31]. Figure 1 shows a scheme of current setup. A simple diagram of the basic dimensions and electric voltages is presented in Fig.2. Clusters were generated in a laser vaporization source by laser ablation of a rotating and translating disk target (diameter 13 mm) with the second harmonic (532 nm) of a nanosecond Nd:YAG laser (Continuum Surelite II-10). Carrier gas was allowed to expand through a pulsed valve (General Valve Series 9) into the source to cool the formed clusters. In this work, the carrier gas (helium) was seeded with water vapor as reactants. The generated clusters passed through a skimmer, and drifted into the extraction region of the reflectron time-of-flight mass spectrometer. The cluster ions (here cations) were extracted and accelerated by pulsed voltages applied on the extraction plates (U_1=1.5 kV, U_2=1.29 kV). The spaces (l_1 and l_2) between the neighbor extraction plates were 30 mm. A horizontal deflector and two sets of Einzel lens were positioned between the extraction plates and the mass gate.

When cluster ions pass the mass gate, the ions of interest can be mass-selected by the mass gate. The mass gate is composed of three plates. A high voltage (+1.7 kV) can be applied to the middle plate, and the other plates are grounded. The high voltage on the middle plates was lowered to ground right before the ion arrival to allow the ions of interest to pass, and was rise up to +1.7 kV immediately after the ions of interest passed through the gate. The precise timing of the mass gated was achieved with a digital delay pulse generator (DG645) and a fast high voltage transistor switch (HTS-31-GSM).

After the ions passed the mass gate, they were decelerated by a decelerator consisting of three plates (D_1, D_2, and D_3) in Fig.2. The first plate D_1 was grounded,

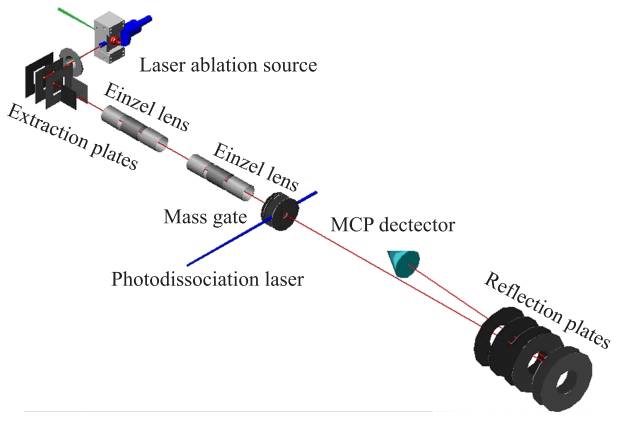

FIG. 1 The scheme of experimental apparatus.

DOI:10.1088/1674-0068/22/06/655-662

a high voltage of U_3=1.067 kV was applied to the second plate D_2, a high voltage of U_4=1.1 kV was applied to the third plate D_3. The decelerated ions were crossed by a pulsed laser at the photodissociation point between plates D_2 and D_3. The laser wavelength can be varied from infrared to ultraviolet depending on the laser systems used. Here, we used the fourth harmonic (266 nm) of a nanosecond Nd:YAG laser (Continuum Surelite II-10) to test the machine. After photodissociation, the parent ions and the fragment ions had the same velocity. And they were reaccelerated by the electric field between plates D_3 and D_4.

After reacceleration, the parent ions and the daughter ions entered the reflectron region, were decelerated and reflected back toward the microchannel plates (MCP) detector. In this course, the reflection angle of the ion flight trajectory is about 5°. After passing through the reflection region, the parent ions and the fragment ions were detected by the MCP detector. The mass signals were amplified with a broadband amplifier, digitized with a 200 MHz digit card, and were collected in a laboratory computer with a home-made time-of-flight (TOF) software.

III. CALCULATIONS OF ION FLIGHT TIME

A. Ion flight under normal conditions (U_3=0, U_4=0)

1. Ion flight time

When we take mass spectrum at normal conditions with the mass gate voltage, U_3 and U_4 equal zero. The flight time of the parent ions at different regions can be calculated with the following equations. The flight time in region l_1 can be represented by t_1:

$$t_1 = \sqrt{\frac{2ml_1d}{q(U_1 - U_2)}} \tag{1}$$

where m is the mass of the parent ion, q is the charge of the parent ion, d is the distance of the parent ion from

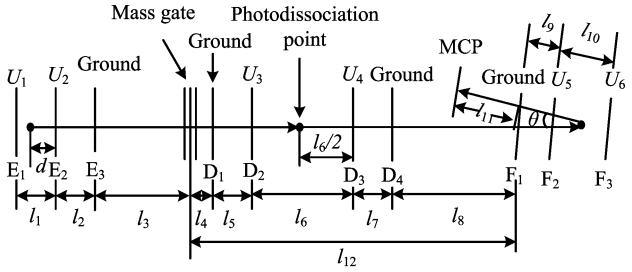

FIG. 2 Simple diagram of the basic dimensions and electric voltages. l_1, l_2=3 mm, d=2 mm, l_3=66.1 mm, l_4=1 mm, l_5=4 mm, l_6=1.8 mm, l_7=4 mm, l_8=67.5 mm, l_9=9.7 mm, l_{10}=13 mm, l_{11}=43.5 mm, and l_{12}=70.2 mm.

Corrections: l_1, l_2=30 mm, d=20 mm, l_3=661 mm, l_4=1 mm, l_5=4 mm, l_6=18 mm, l_7=4 mm, l_8=675 mm, l_9=97 mm, l_{10}=130 mm, l_{11}=435 mm, and l_{12}=702 mm.

plate E_2, U_1 and U_2 are the electric voltages applied to extraction plates E_1 and E_2 (Fig.2).

The flight time in region l_2 and l_3 can be represented by t_2 and t_3:

$$t_2 = \frac{l_2}{U_2}\sqrt{\frac{2m}{ql_1}}\left[\sqrt{(l_1-d)\,U_2+dU_1}-\sqrt{d(U_1-U_2)}\right] \quad (2)$$

$$t_3 = \frac{l_3}{\sqrt{q}\sqrt{\dfrac{2(l_1-d)U_2+2dU_1}{ml_1}}} \quad (3)$$

The flight time between the mass gate and the reflectron plate F_1 can be denoted by t_4:

$$t_4 = \frac{l_{12}}{\sqrt{q}\sqrt{\dfrac{2(l_1-d)U_2+2dU_1}{ml_1}}} \quad (4)$$

The flight time inside the reflectron in region l_9 and l_{10} in one direction can be represented by t_5 and t_6 respectively:

$$t_5 = \frac{l_9}{U_5\cos(\theta/2)}\sqrt{\frac{2m}{ql_1}}\Big[\sqrt{(l_1-d)\,U_2+dU_1}- \sqrt{(l_1-d)\,U_2+dU_1-l_1U_5}\Big] \quad (5)$$

$$t_6 = \frac{l_{10}}{(U_6-U_5)\cos(\theta/2)}\sqrt{\frac{2m}{ql_1}}\cdot \sqrt{(l_1-d)\,U_2+dU_1-l_1U_5} \quad (6)$$

The flight time between the reflectron plate F_1 and the MCP detector can be represented by t_7:

$$t_7 = \frac{l_{11}}{\sqrt{q}\sqrt{\dfrac{2(l_1-d)U_2+2dU_1}{ml_1}}} \quad (7)$$

The total flight time of the ions from the extraction region to the MCP detector can be calculated with Eq.(8):

$$t_{\text{total}} = t_1+t_2+t_3+t_4+2t_5+2t_6+t_7 \quad (8)$$

2. First space focus

In order to gain better mass selection, we adjusted the extraction voltages, U_1 and U_2, to set the first focus space point to the position of the mass gate. The flight time for the ions from the extraction region to the mass gate can be determined with the following equation:

$$t_{\text{focus1}} = t_1+t_2+t_3 \quad (9)$$

where the detailed calculations of t_1, t_2, and t_3 have been given in Eqs. (1), (2), and (3). Assuming two ions of the same mass originated from two different positions at the extraction region, and their distances from plate E_2 are d' and d'' respectively (Fig.2). Their flight times from the extraction region to the mass gate (the first space focus point) are t'_{focus1} and t''_{focus1}. We have Eq.(10) at the first space focus point.

$$\begin{aligned} &t'_{\text{focus1}} = t''_{\text{focus1}} \\ &t'_1+t'_2+t'_3 = t''_1+t''_2+t''_3 \end{aligned} \quad (10)$$

Based on Eq.(10), we found that the first space focus can be achieved at the position of the mass gate by setting U_1 and U_2 to 1.5 and 1.29 kV respectively.

3. Second space focus

The flight time for the ions from the first space focus point to the MCP detector can be determined with the following equation:

$$t_{\text{focus2}} = t_4+2t_5+2t_6+t_7 \quad (11)$$

where the detailed calculations of t_4, t_5, t_6, and t_7 have been give in Eqs. (4), (5), (6), and (7).

Similar to the calculations of the first space focus, assuming two ion of the same mass originated from two different positions at the extraction region, and their distances from plate E_2 are d' and d'' respectively (Fig.2). Their flight times from the first space focus point to the MCP detector are t'_{focus2} and t''_{focus2}. We have Eq.(12) when the second space focus is accomplished.

$$\begin{aligned} &t'_{\text{focus2}} = t''_{\text{focus2}} \\ &t'_4+2t'_5+2t'_6+t'_7 = t''_4+2t''_5+2t''_6+t''_7 \end{aligned} \quad (12)$$

Since the extraction voltages, U_1 and U_2, have been determined with Eq.(10). The voltages on the reflectron plates, U_5 and U_6, can be adjusted to achieve the second space focus at the MCP detector. Based on Eq.(12), we calculated that the voltages for U_5 and U_6 are 0.902 and 1.7 kV respectively for the second space focus. During the tuning up of our instrument, we found the best resolution can be obtained by setting U_5 and U_6 to be 1.085 and 1.7 kV respectively. The experimental value of U_5 is about 180 V higher than the calculated value. That probably is due to the uncertainties in the distances between the reflectron plates. U_5 needs to be adjusted slightly in the photodissociation experiment when the voltages U_3 and U_4 are applied.

4. Test experiments

Figure 3 shows the typical mass spectra taken on our machine with U_1, U_2, U_5, and U_6, equal 1.5, 1.29, 1.085, and 1.7 kV respectively. The full width at half maximum(FWHM) of the Co^+ mass peak is about 0.034 a.u.. That gives a mass resolution of

DOI:10.1088/1674-0068/22/06/655-662

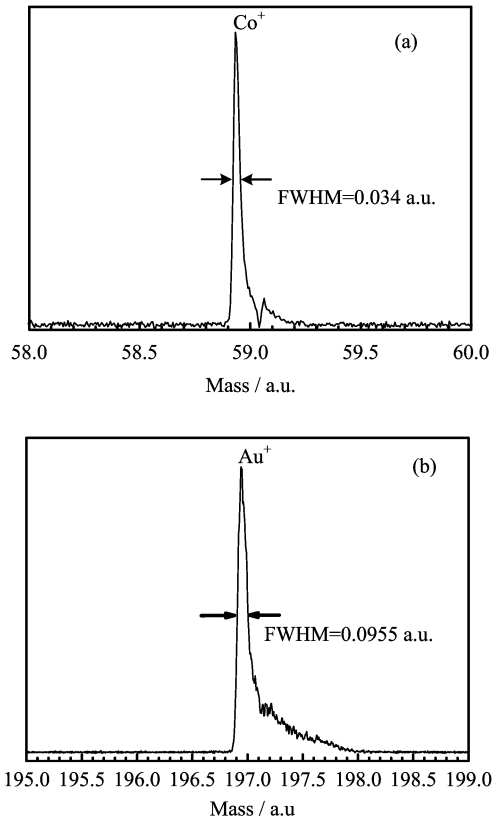

FIG. 3 Mass spectra of Co^+ (a) and Au^+ (b) generated by laser ablation.

$m/\Delta m$=1730. The FWHM of the Au^+ mass peak is about 0.0955 a.u.. The mass resolution of the Au^+ peak is about 2070. These values are similar to the best mass resolution of 1930 reported previously [31].

B. Ion flight time in photodissociation experiments

1. Parent Ions

For the photodissociation experiments, the parent ions can be selected by the mass gate and decelerated by the voltages applied to plates D_2 and D_3 (Fig.2). When the parent ions reach the photodissociation point, their velocity can be expressed with the following equation:

$$v = \sqrt{\frac{2q}{ml_1}}\sqrt{(l_1-d)U_2 + dU_1 - \frac{l_1}{2}(U_3+U_4)} \quad (13)$$

After the mass-selection, we can start to take mass spectrum of the parent ions and daughter ions using the photodissociation point as the start point. In this case, the fire time of the photodissociation laser should be considered as time zero.

The flight time of the parent ions from the photodissociation point to plate D_3 can be denoted with t_{p1}:

$$t_{p1} = \sqrt{\frac{ml_1}{2q}}l_6\left[\sqrt{(l_1-d)U_2 + dU_1 - \frac{l_1}{2}(U_3+U_4)} + \sqrt{(l_1-d)U_2 + dU_1 - l_1U_4}\right]^{-1} \quad (14)$$

The flight time of the parent ions from plate D_3 to plate D_4 can be expressed with t_{p2}:

$$t_{p2} = \frac{l_7}{U_4}\sqrt{\frac{2m}{ql_1}}\left[\sqrt{(l_1-d)U_2 + dU_1} - \sqrt{(l_1-d)U_2 + dU_1 - l_1U_4}\right] \quad (15)$$

The flight time of the parent ions from plate D_4 to plate F_1 can be represented with t_{p3}:

$$t_{p3} = \frac{l_8}{\sqrt{q}\sqrt{\frac{2(l_1-d)U_2 + 2dU_1}{ml_1}}} \quad (16)$$

The flight time of the parent ions from plate F_1 to plate F_2 can be represented with t_{p4}:

$$t_{p4} = \frac{l_9}{U_5\cos(\theta/2)}\sqrt{\frac{2m}{ql_1}}\left[\sqrt{(l_1-d)U_2 + dU_1} - \sqrt{(l_1-d)U_2 + dU_1 - l_1U_5}\right] \quad (17)$$

The flight time of the parent ions from plate F_2 to the turning point of their trajectory can be represented with t_{p5}:

$$t_{p5} = \frac{l_{10}}{(U_6-U_5)\cos(\theta/2)}\sqrt{\frac{2m}{ql_1}}\cdot\sqrt{(l_1-d)U_2 + dU_1 - l_1U_5} \quad (18)$$

The flight time of the parent ions from plate F_1 to the MCP detector can be represented with t_{p6}:

$$t_{p6} = \frac{l_{11}}{\sqrt{q}\sqrt{\frac{2(l_1-d)U_2 + 2dU_1}{ml_1}}} \quad (19)$$

The total flight time of the parent ions from the photodissociation point to the MCP detector can be denoted with the following equation:

$$t_p = t_{p1} + t_{p2} + t_{p3} + 2t_{p4} + 2t_{p5} + t_{p6} \quad (20)$$

2. Daughter ions

The initial velocity of the daughter ions at the photodissociation point is the same as that of the parent

DOI:10.1088/1674-0068/22/06/655-662

ions (see Eq.(13)). Since the daughter ions have smaller mass than the parent ions, their initial kinetic energy is smaller than the parent ions. After reaccelerated by the electric field applied between plates D_3 and D_4, the overall kinetic energy of the daughter ions is still smaller than that of the parent ions. Due to the different kinetic energies between the daughter ions and parent ions, their flight time should be calculated with different equations. Here we present calculations of the daughter ion flight time from the photodissociation point to the MCP detector.

To differentiate the symbols between the parent ion flight time and daughter ion flight time, we use t_f to designate the flight time of the daughter ions (fragments).
(i) The flight time in the photodissociation region $l_6/2$:

$$t_{f1}=\frac{l_6}{\sqrt{q}}\left[\sqrt{\frac{2\left(l_1-d\right)U_2+2dU_1-l_1\left(U_3+U_4\right)}{ml_1}}+\sqrt{\frac{2\left(l_1-d\right)U_2+2dU_1-l_1\left(U_3+U_4\right)}{ml_1}-\frac{U_4-U_3}{m_f}}\right]^{-1} \tag{21}$$

where m_f is the daughter ion mass, m is the parent ion mass.
(ii) The flight time in the reacceleration region l_7:

$$t_{f2}=\frac{m_f l_7}{\sqrt{q}U_4}\left\{\left[\frac{U_3+U_4}{m_f}+\frac{2(l_1-d)U_2+2dU_1-l_1\left(U_3+U_4\right)}{ml_1}\right]^{1/2}-\left[\frac{2(l_1-d)U_2+2dU_1-l_1\left(U_3+U_4\right)}{ml_1}-\frac{U_4-U_3}{m_f}\right]^{1/2}\right\} \tag{22}$$

(iii) The flight time in the region l_8:

$$t_{f3}=\frac{l_8}{\sqrt{q}}\left[\frac{U_3+U_4}{m_f}+\frac{2(l_1-d)U_2+2dU_1-l_1(U_3+U_4)}{ml_1}\right]^{-1/2} \tag{23}$$

(iv) The flight time in the reflection region l_9:

$$t_{f4}=\frac{m_f l_9}{\sqrt{q}U_5\cos(\theta/2)}\left\{\left[\frac{U_3+U_4}{m_f}+\frac{2(l_1-d)U_2+2dU_1-l_1(U_3+U_4)}{ml_1}\right]^{1/2}-\left[\frac{U_3+U_4-2U_5}{m_f}+\frac{2(l_1-d)U_2+2dU_1-l_1(U_3+U_4)}{ml_1}\right]^{1/2}\right\} \tag{24}$$

(v) The flight time from plate F_2 to the turning point of the daughter ion trajectory (in region l_{10}) :

$$t_{f5}=\frac{m_f l_{10}}{\sqrt{q}\left(U_6-U_5\right)\cos\left(\theta/2\right)}\left[\frac{U_3+U_4-2U_5}{m_f}+\frac{2(l_1-d)U_2+2dU_1-l_1\left(U_3+U_4\right)}{ml_1}\right]^{1/2} \tag{25}$$

(vi) The flight time in the region l_{11}:

$$t_{f6}=\frac{l_{11}}{\sqrt{q}}\left[\frac{U_3+U_4}{m_f}+\frac{2(l_1-d)U_2+2dU_1-l_1\left(U_3+U_4\right)}{ml_1}\right]^{-1/2} \tag{26}$$

The total daughter ion flight time from the photodissociation point to the MCP detector can be denoted with the following equation:

$$t_f=t_{f1}+t_{f2}+t_{f3}+2t_{f4}+2t_{f5}+t_{f6} \tag{27}$$

C. Calibration of m_f

Based on Eq.(13), the initial kinetic energy of the parent ions at the photodissociation point can be expressed by the following equation:

$$E_k=\frac{q}{l_1}\left[(l_1-d)U_2+dU_1-\frac{l_1}{2}\left(U_3+U_4\right)\right] \tag{28}$$

The initial velocity of the daughter ions at the photodissociation point is the same as that of the parent ions (see Eq.(13)). Thus, the initial kinetic energy of the daughter ions E_{kf} equals $m_f E_k/m$ at the photodissociation point. After reaccelerated by the electric field applied between plates D_3 and D_4, the overall kinetic energy of the daughter ions is still smaller than that of the parent ions, which means the velocity of the daughter ions is slower than it is supposed to be.

As we know, for the parent ions, t_p is proportional to $\sqrt{m}$. However, that is not the case for the daughter ions since the initial and total kinetic energy of the daughter ions depends on the mass of the daughter ions. Thus, we need to pay special attention to the calibration of daughter ion mass (m_f).

DOI:10.1088/1674-0068/22/06/655-662

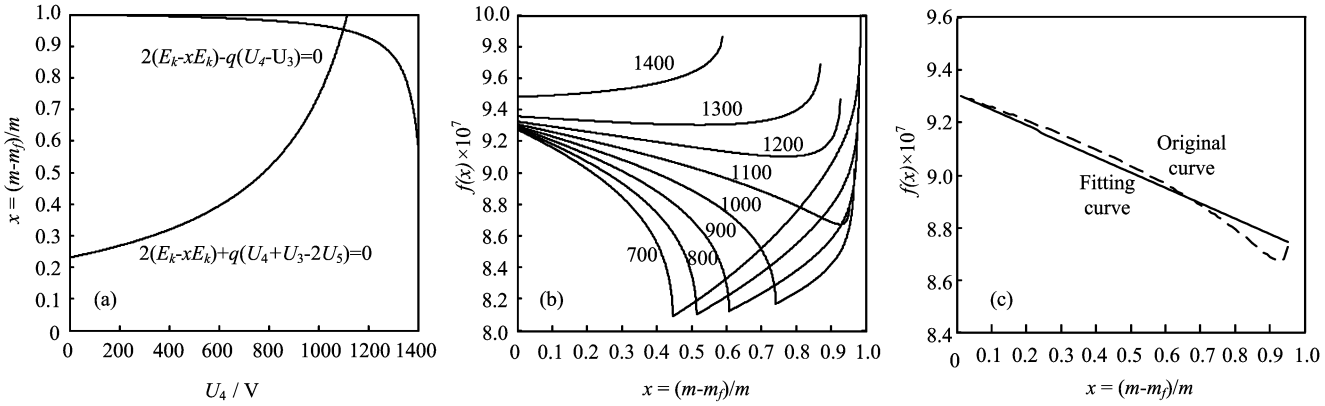

FIG. 4 (a) Curves with x as the ordinate and U_4 as the abscissa (note that E_k changes with U_4). (b) $f(x)$ versus x at different deceleration (U_4 and reacceleration conditions (U_5=1.1 kV and U_6=1.7 kV). (c) Linear fit of $f(x)$ curve with U_4=U_5=1.1 kV and U_6=1.7 kV.

Since E_{kf}=$m_f E_k/m$, we can get the following equation:

$$\frac{E_{kf}}{m_f}=\frac{E_k}{m}=\frac{q}{ml_1}\left[(l_1-d)U_2+dU_1-\frac{l_1}{2}(U_3+U_4)\right] \quad (29)$$

And we can get Eq.(30) by substituting term $\frac{q}{ml_1}\left[(l_1-d)U_2+dU_1-\frac{l_1}{2}(U_3+U_4)\right]$ with $\frac{E_{kf}}{m_f}$ in the Eqs.(21)−(26).

$$t_f=\sqrt{m_f}\left\{\frac{l_8+l_{11}}{\sqrt{2E_{kf}+q(U_3+U_4)}}+\frac{1}{q}\cdot\left[\frac{ql_6}{\sqrt{2E_{kf}}+\sqrt{2E_{kf}-q(U_4-U_3)}}+\frac{l_7}{U_4}\cdot\left(\sqrt{2E_{kf}+q(U_3+U_4)}-\sqrt{2E_{kf}-q(U_4-U_3)}\right)+\frac{2l_9}{U_5\cos(\theta/2)}\left(\sqrt{2E_{kf}+q(U_3+U_4)}-\sqrt{2E_{kf}+q(U_3+U_4-2U_5)}\right)+\frac{2l_{10}\sqrt{2E_{kf}+q(U_3+U_4-2U_5)}}{(U_6-U_5)\cos(\theta/2)}\right]\right\} \quad (30)$$

If we define $(m-m_f)/m=x$, then we can get E_{kf}=$(1-x)E_k$. Subsequently, we can write t_f as a function of x by replacing E_{kf} with $(1-x)E_k$ in Eq.(30). It can be written as the following:

$$t_f=f(x)\sqrt{m_f} \quad (31)$$

where function $f(x)$ can be expressed by Eq.(32).

$$f(x)=\frac{l_8+l_{11}}{\sqrt{2(E_k-xE_k)+q(U_3+U_4)}}+\frac{1}{q}\cdot\left\{\frac{ql_6}{\sqrt{2(E_k-xE_k)}+\sqrt{2(E_k-xE_k)-q(U_4-U_3)}}+\frac{l_7}{U_4}\left[\sqrt{2(E_k-xE_k)+q(U_3+U_4)}-\sqrt{2(E_k-xE_k)-q(U_4-U_3)}\right]+\frac{2l_9}{U_5\cos(\theta/2)}\cdot\left[\sqrt{2(E_k-xE_k)+q(U_3+U_4)}-\sqrt{2(E_k-xE_k)+q(U_3+U_4-2U_5)}\right]+\frac{2l_{10}\sqrt{2(E_k-xE_k)+q(U_3+U_4-2U_5)}}{(U_6-U_5)\cos(\theta/2)}\right\} \quad (32)$$

When the value of U_1 and U_2 is fixed, the initial kinetic energy of the parent ions (E_k) at the photodissociation point depends on U_3 and U_4. In our case, we set U_3=$0.97U_4$. Therefore, the shape of $f(x)$ curve depends on U_4. From Eq.(32), we can see the daughter ions cannot reach the MCP detector when $2(E_k-xE_k)-q(U_4-U_3)\leq 0$ because they cannot fly out of region l_6. When $2(E_k-xE_k)+q(U_4+U_3-2U_5)\leq 0$, the daughter ions cannot reach region l_{10}. However, they still can make turns in region l_9 and fly toward the MCP detector. Figure 4(a) shows the curves of $2(E_k-xE_k)-q(U_4-U_3)=0$ and $2(E_k-xE_k)+q(U_4+U_3-2U_5)=0$ with x as the ordinate and U_4 as the abscissa.

When $2(E_k-xE_k)+q(U_4+U_3-2U_5)\leq 0$, the formula of $f(x)$ can be changed to the following:

$$f(x)=\frac{l_8+l_{11}}{\sqrt{2(E_k-xE_k)+q(U_3+U_4)}}+\frac{1}{q}\cdot\left\{\frac{ql_6}{\sqrt{2(E_k-xE_k)}+\sqrt{2(E_k-xE_k)-q(U_4-U_3)}}+\frac{l_7}{U_4}\left[\sqrt{2(E_k-xE_k)+q(U_3+U_4)}-\right.\right.$$

DOI:10.1088/1674-0068/22/06/655-662

$$\sqrt{2(E_k - xE_k) - q(U_4 - U_3)}\Big] + \frac{2l_9\sqrt{2(E_k - xE_k) + q(U_3 + U_4)}}{U_5\cos(\theta/2)}\Bigg\} \quad (33)$$

Based on Eqs. (32) and (33), we can generate the $f(x)$ curves at different U_4 values. The results are shown in Fig.4(b). From Fig.4 (a) and (b), we can see that the light daughter ions cannot be detected when U_4 is very high. We found that U_4 equals 1100 V is suitable for our experiments since the masses of the daughter ions in our experiments are over 5% of that of the parent ions. Note, the voltages U_3 and U_4 has to be adjusted in order to detect the daughter ions with mass lower than 5% of the parent ion mass. The detection of light daughter ions can be improved by reducing the difference between U_3 and U_4.

In Fig.4(c), the $f(x)$ curve is approximately a straight line when x is smaller than 0.95. Therefore, we can fit this curve with a straight line using Eq.(34).

$$f(x) = a(1 - cx) \quad (x \le 0.95) \quad (34)$$

By fitting the first part of the curve ($x \le 0.95$) with Eq.(34), we obtained the equation:

$$f(x) = 9.306 \times 10^7(1 - 0.0656x) \quad (x \le 0.95) \quad (35)$$

Thus, the daughter ion flight time can be expressed as the following equation:

$$t_f = a\left(1 - c\frac{m - m_f}{m}\right)\sqrt{m_f}, \quad \left(\frac{m - m_f}{m} \le 0.95\right) \quad (36)$$

where a and c are constants, m_f is the daughter ion mass, and m is the parent ion mass. In our experimental conditions, a=9.306×10^7 s·kg$^{-1/2}$, and c equals 0.0656. The value of c=0.0656 means that the error in the daughter ion mass is under 6.6% if we omit c in Eq.(36). By including c in Eq.(36), the error can be reduced to 0.5%. From Eq.(36), we can see that t_f=$a\sqrt{m_f}$ when m_f=m, which is consistent with the flight time of parent ions. The calibration of daughter ion mass can be easily implemented with computer programming by using Eq.(36).

D. Test experiments

Figure 5 shows the photodissociation mass spectra of $Co(H_2O)_2^+$ and $Co(H_2O)_3^+$ clusters obtained in the test experiments. In Fig.5(a), the mass resolution ($m/\Delta m$) for the mass peak of daughter ion $CoOH^+$ is about 240. In Fig.5(b), the mass resolution ($m/\Delta m$) for the peak of daughter ion $Co(H_2O)^+$ is about 160. We are able to distinguish between $CoOH^+$ and $Co(H_2O)^+$ daughter ions in both photodissociation mass spectra. The daughter ion mass resolution is better than those in the literature. That proves that the principle

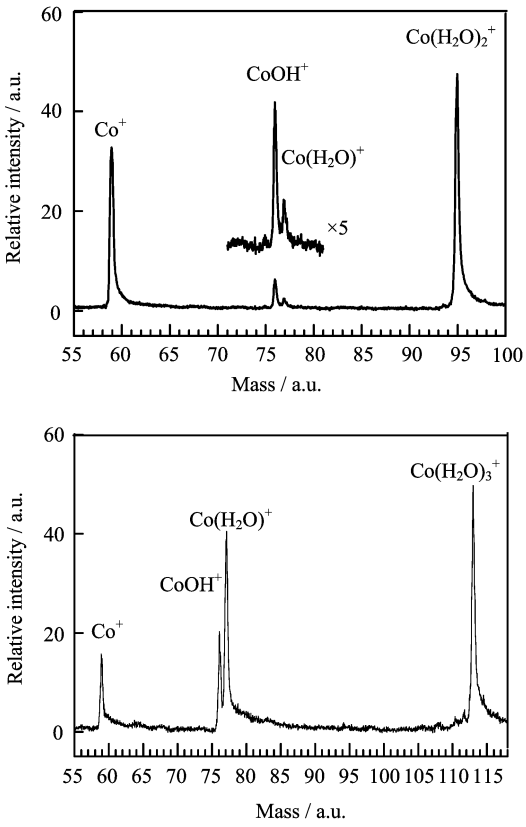

FIG. 5 Photodissociation mass spectra of $Co(H_2O)_2^+$ and $Co(H_2O)_3^+$ clusters.

of our selection-deceleration-dissociation-reacceleration method works. The instrument can still be improved in the future based on this method. Note, it is normal that the resolution of photodissociation mass spectra (Fig.5) is worse than the total mass resolution of reflectron time-of-flight mass spectrometer (RTOF-MS) (Fig.3) since the flight path of the daughter ions is much shorter.

IV. CONCLUSION

We developed a selection-deceleration-dissociation-reacceleration method for laser photodissociation of mass-selected cluster ions using RTOF-MS. With this method, the parent ions were selected by a mass gate near the first space focus point and decelerated immediately after the mass gate, were then crossed by a laser beam for dissociation. The daughter ions and surviving parent ions were re-accelerated and analyzed by the reflectron time-of-flight mass spectrometer. We presented the calculations for the flight times of parent and daughter ions. We also proposed a equation for the mass calibration of daughter ions. The test experiments show that the principle of our selection-deceleration-dissociation-reacceleration method is cor-

DOI:10.1088/1674-0068/22/06/655-662

rect. However, the test results shown here have not reached the upper limit of our apparatus yet. Based on the selection-deceleration-dissociation-reacceleration method, the apparatus can still be improved in the future.

V. ACKNOWLEDGMENTS

This work was supported by the National Natural Science Foundation of China (No.20853001). We thank Professor Qi-he Zhu and Professor Zhen Gao for valuable discussions.

[1] B. A. Mamyrin, V. I. Karataev, D. V. Shmikk, and V. A. Zagulin, Zh. Eksp. Teor. Fiz. **64**, 82 (1973).
[2] D. M. Lubman, W. E. Bell, and M. N. Kronick, Anal. Chem. **55**, 1437 (1983).
[3] J. Grotemeyer, U. Bosel, K. Walter, and E. W. Schlag, J. Am. Chem. Soc. **108**, 4233 (1986).
[4] K. Laihing, R. G. Wheeler, W. L. Wilson, and M. A. Duncan, J. Chem. Phys. **87**, 3401 (1987).
[5] M. A. Elsayed and T. L. Tai, J. Phys. Chem. **92**, 5333 (1988).
[6] K. F. Willey, P. Y. Cheng, T. G. Taylor, M. B. Bishop, and M. A. Duncan, J. Phys. Chem. **94**, 1544 (1990).
[7] R. Tembreull and D. M. Lubman, Anal. Chem. **58**, 1299 (1986).
[8] W. F. Haddon and Fw. McLaffer, Anal. Chem. **41**, 31 (1969).
[9] G. M. Neumann, M. M. Sheil, and P. J. Derrick, Z. Naturforsch. Teil. A **39**, 584 (1984).
[10] P. J. Brucat, L. S. Zheng, C. L. Pettiette, S. Yang, and R. E. Smalley, J. Chem. Phys. **84**, 3078 (1986).
[11] Y. Liu, Q. L. Zhang, F. K. Tittel, R. F. Curl, and R. E. Smalley, J. Chem. Phys. **85**, 7434 (1986).
[12] J. P. Kiplinger and M. M. Bursey, Org. Mass Spectrom. **23**, 342 (1988).
[13] N. E. Levinger, D. Ray, M. L. Alexander, and W. C. Lineberger, J. Chem. Phys. **89**, 5654 (1988).
[14] L. A. Posey and M. A. Johnson, J. Chem. Phys. **89**, 4807 (1988).
[15] K. Laihing, P. Y. Cheng, T. G. Taylor, K. F. Willey, M. Peschke, and M. A. Duncan, Anal. Chem. **61**, 1458 (1989).
[16] P. Y. Cheng, K. F. Willey, J. E. Salcido, and M. A. Duncan, Int. J. Mass Spectrom. Ion Process **102**, 67 (1990).
[17] J. M. Papanikolas, J. R. Gord, N. E. Levinger, D. Ray, V. Vorsa, and W. C. Lineberger, J. Phys. Chem. **95**, 8028 (1991).
[18] R. Bouyer, F. Roussel, P. Monchicourt, M. Perdrix, and P. Pradel, J. Chem. Phys. **100**, 8912 (1994).
[19] T. G. Dietz, M. A. Duncan, D. E. Powers, and R. E. Smalley, J. Chem. Phys. **74**, 6511 (1981).
[20] N. R. Walker, G. A. Grieves, R. S. Walters, and M. A. Duncan, Chem. Phys. Lett. **380**, 230 (2003).
[21] T. D. Jaeger and M. A. Duncan, Int. J. Mass Spectrom. **241**, 165 (2005).
[22] E. D. Pillai, T. D. Jaeger, and M. A. Duncan, J. Phys. Chem. A **109**, 3521 (2005).
[23] V. Kasalova, W. D. Allen, H. F. Schaefer, E. D. Pillai, and M. A. Duncan, J. Phys. Chem. A **111**, 7599 (2007).
[24] Z. A. Reed and M. A. Duncan, J. Phys. Chem. A **112**, 5354 (2008).
[25] J. Velasquez, B. Njegic, M. S. Gordon, and M. A. Duncan, J. Phys. Chem. A **112**, 1907 (2008).
[26] D. W. Boo, Y. Ozaki, L. H. Andersen, and W. C. Lineberger, J. Phys. Chem. A **101**, 6688 (1997).
[27] D. S. Cornett, M. Peschke, K. Laihing, P. Y. Cheng, K. F. Willey, and M. A. Duncan, Rev. Sci. Instrum. **63**, 2177 (1992).
[28] L. N. Ding, M. A. Young, P. D. Kleiber, W. C. Stwalley, and A. M. Lyyra, J. Phys. Chem. **97**, 2181 (1993).
[29] J. Husband, F. Aguirre, P. Ferguson, and R. B. Metz, J. Chem. Phys. **111**, 1433 (1999).
[30] Y. S. Yang and C. S. Yeh, Chem. Phys. Lett. **305**, 395 (1999).
[31] X. P. Xing, Z. X. Tian, P. Liu, Z. Gao, Q. H. Zhu, and Z. C. Tang, Chin. J. Chem. Phys. **15**, 83 (2002).

DOI:10.1088/1674-0068/22/06/655-662